Experimental and Numerical Investigations on Fully nonlinear free surface waves

1.0 Introduction

The simulation of nonlinear waves has been carried out successfully by most of the researchers. The results have been reported so far in the literature is simply based on qualitative comparison; none of them reveal the numerical and physical phase difference for nonlinear waves. In this paper, the simulation of nonlinear waves using Finite Element procedure is investigated by using the two different velocity recovery techniques (Cubic Spline and Least square) and compared with the experimental measurement. The analysis has been carried out using the wavelet transformations, which gives clear understanding between the numerical and the experimental results with respect to the time-frequency space, when compared to the traditional Fourier transformation. The analysis reveals that the velocity recovery technique based on Cubic spline leads to higher phase difference for steep waves, whereas for small steep waves both Least square and cubic spline gives identical results. More over, the phase difference exists not at the primary period under consideration but at the lower mode. Apart from the qualitative results based on Wavelets, quantitative results for phase angles are carried for regular and Cnoidal wave. PIV measurements for solitary wave and its comparison with the numerical simulation were also carried out.

2.0 Experimental details

The experiments were carried out in the wave Flume at Franzius-Institute, University of Hannover,Germany. The flume is 100m long with the width of 2m and 4m deep. The water depth for the present study is 0.61m. The existing system of water circulation to cool the wave paddle to avoid friction at the side wall is not working properly; hence by using external pipe water is poured on the side of the wave paddle leading to increase in water level. It has been noticed over a day that the increase in water level is roughly 2 cm, so measurement of water depth is carried out before every run. This plays a major role in the numerical simulation, if the water depth changes then one cannot have an exact comparison and interpretation with the experimental measurements. There are six wave gauges being deployed in the wave flume at 4.8495m, 20.146m, 25.136m, 30.425m, 40.406m and 50.609m from the

wave paddle. The distances are being measured using laser distometer. The input to the numerical model is from the feedback signal of the physical wave paddle. The input signal, water depth and the location of the measurement of time histories for a particular run are important part in the experiments to compare with the numerical simulation and to analyse the results. The generations of regular waves and Cnoidal waves have been carried out in this flume. For the generation of Solitary waves, the experiments were carried out at IGAW Wave Flume, University of Wuppertal. The length of this flume is 24m with the width of 0.3m and 0.5m deep. The water depth is 0.2145m for the studies carried out. The flume is equipped with the digital motor signal to the wave paddle with high precision. The wave histories are recorded at 1.743m and at 6.74m using Ultrasonic sensors. The PIV measurements are carried out using the high Speed CCD camera at 3.45m having the resolution of 256 x256 pixels. The PIV setup is shown in Fig.1

3.0Wavelet Analysis

The analysis of the numerical and experimental time series has been carried out using the wavelet analysis. In this section, a brief overview about Wavelet is given. The description about Wavelets are given by Weng and Lau(1995), Torrence and Compo (1997) and the theoretical background of wavelet analysis are described in Daubechies (1990). This is a suitable tool for the analysis of the transient, non-stationary or time-varying phenomena. In the context of ocean Engineering, the wavelet transform has been successfully used in the dispersion of ocean waves by Meyers *et al.,*(1993), wave growth and breaking by Liu(1994) on the prediction of the ocean waves using data buoy. Wavelets are similar to but an extension of Fourier analysis and computational wise the wavelet transformation are similar to the fast fourier transformation and hence its an alternative to classical windowed fourier transformation. The major difference when compared to the windowed fourier transformation is that the window in wavelet is already oscillating and is called mother wavelet, which are not multiplied by sine or cosine functions.

4.0 Results and Discussions

4.1. Regular Wave

The test has been carried out for the wave period of 1.92s, with two different wave heights, one corresponds to small steep waves of 0.01 and the other corresponds

to medium steep waves of 0.047. In numerical modeling the number of nodes used in the horizontal direction and vertical directions are 1101 and 17 respectively. For the case of Cubic Spline approach there is no regridding is applied, whereas, the regridding has been carried out for every 40 time steps. The time step used for the calculations are 0.02s. The numerical setup is kept constant for all the cases, unless and otherwise quoted. The comparison between the experimental and two different numerical procedures time histories at various locations along the length of the tank for small steep waves (wave height of 0.02m) are shown in Fig.2. The input velocity obtained from differentiating the measured paddle displacement, there are some noises in the signal as shown in Fig.2a. The time series are shown only at three locations for all the cases reported herein. The figure shows the excellent comparison between the numerical approaches based on cubic spline (CS) and least square (LS) method with that of experimental measurements (EXP). The wave spectral analysis for the time histories near to the paddle and far away from the paddle is depicted in Fig.3a and b. The wavelet power spectra for the experimental measurements alone are shown in Fig.3c and d. The figure shows the wave period is around 1.92s, the COI where edge effects might have influence is shown as a lighter shade(the values within this region is presumably reduced in magnitude due to zero padding), the thick black contour designates the 95% confidence level against red noise. In order to uncover the difference between the two time histories near to the paddle, the cross wavelet power and phase difference are shown in Fig.4a and b for EXP x CS and EXP x LS. The arrows indicates the relative phase difference between the two time series, the arrows pointing to the right indicates the in-phase, left arrows indicates out of phase and the arrows pointing downward indicates that the numerical method leads the experiments by 90^0. The figure shows that within the 95% confidence contours, the time series are in phase with the experiments. The quantitative mean phase angle in the XWT for EXP x CS is $-2.28^0 \pm 1.571^0$ ($\pm$ indicates error estimated using the circular standard deviation), whereas for EXP x LS is $-2.49^0 \pm 1.470^0$. The cross wavelet shows the high common power exists between the two time series, in order to reveal the phase lock behaviour the wave coherent transform is used. The squared wavelet coherent transform for EXP x CS and EXP x LS are shown in Fig. 4c and 4d. The area of the 95% confidence contour is large when compared to the cross wavelet power, showing the intensity of covariance irrespective of high common power. The figure shows that

the significant wavelet coherence exists for the wave period below 1s. The arrows indicate that in the region of primary frequency, the time series are in-phase and scattered elsewhere. The mean phase angle for squared WTC of EXP x CS and EXP x LS are $-1.82^0 \pm 39.73^0$ and $-1.36^0 \pm 37.08^0$, respectively. Moreover, the phase angle is not constant over the length of the tank, the reason might be due to the fact, that it is difficult to measure the location of the experimental wave gauges in the long flume accurately (even 5cm of error leads to deviation), hence it is mostly the experimental difficulties. Probable reason for the small deviation in the lower period may be due to the fact, that the input signal (paddle displacement) obtained from the paddle for the low period range may exhibit noisy signal when one differentiate to obtained velocity (input for the numerical code).

The quantitative mean phase angles for all the test cases regular and Cnoidal waves are reported in Table 1.The tables reveals that for small wave steepness, the phase difference is small, while for the medium wave steepness, the phase difference is very high for CS when compared to LS. Moreover, the phase angle is not constant over the length of the tank, the reason might be due to the fact, that it is difficult to measure the location of the experimental wave gauges in the long flume accurately (even 5cm of error leads to deviation), hence it is mostly the experimental difficulties. Probable reason for the small deviation in the lower period may be due to the fact, that the input signal (paddle displacement) obtained from the paddle for the low period range may exhibit noisy signal when one differentiate to obtained velocity (input for the numerical code). The more detail about the experiments and the wavelet analysis can be found in Sriram et al. (2008).

4.3. Solitary Wave and PIV measurements

Due to the limitation of the wave paddle at Franzuis-Institute, the generation of solitary waves has been carried out at IGAW, Wuppertal. The generation of solitary waves by prescribing the 'piston' wave maker motion is determined from the first order Boussinesq wave theory used by Goring (1979). Using the present equations the generation of solitary waves has been carried out and the surface profile has been measured using ultrasonic probe at two locations. the experiments are carried out for H/d = 0.1 to 0.4 and measured wave height is compared with the numerical simulation(LS) as shown in Fig.5a-d, from the figure it is clearly noticed that the

measured wave height is small and the profile is different when one compares to the numerical simulation for smaller steepness, whereas for steep waves, even though the wave height remains the same but the width of the solitons are small, the reason is the mass of the water that is generating is different, even though the paddle signal is exactly the same (comparison not shown). The loss of volume of water is due to the fact that the water is flowing backward of the paddle when it starts generating, through the gap between the wave paddle and the side walls. The width of the flume is very small, so this effect is more pronounced. The reason for the wave height remains unchanged for the steeper ones are owing to the fact that the time of stroke is very fast, when compared to smaller steepness. Since the width of the profile is small, the waves are become unstable and lead to trough formation (more trailing waves than expected). This feature has been captured using the high speed camera and the various snap shots of the water flowing through the gaps are shown in Fig.6. One can minimize this effect by adjusting the input signal to generate the target wave height and profile using trial and error method. The input signal for the numerical model (i.e., the real one) and the signal given to the paddle (i.e., based on trial and error) to generate a same wave height is shown in Fig.7for H/d = 0.1. Since, the incident profile is matched near to the paddle and comparison is made at the second location, the wavelet analysis is not carried out. The comparison between the numerical simulations (both approaches) and experimental measurements for steepness ranging from 0.1 to 0.5 are shown in Fig.8. The numbers of nodes in the horizontal and vertical direction used in the numerical modeling are 601 and 17 respectively. From the Figure, one can note another interesting feature that after the main wave passes, the oscillation is below the zero level, which once again proves that the water is flowing back through the side of the wave paddle after reaching the extreme position of the input signal. This will eventually reduce the trailing waves that should be presented in solitary wave generation, but actually there are lots of researches on this topic of minimization of trailing waves. Thus, in higher wave steepness, one could clearly see that the numerical simulation and experimental measurement have difference in comparison for trailing waves. The Figure also shows that the Cubic spline is having phase difference for steepness above 0.4. In order to reveal the velocity information, due to which the phase difference exist. The PIV measurements are carried out and the details are given in the following paragraph.

The camera is placed at 1.45m (focus) from the center of the flume, it should be noted that the minimum focusing distance should be 1m. So, for small steepness waves of 0.1, we have found lots of noise in the data, leading to spurious velocity information. The field of View (FOV) is 0.26 x 0.26m. The sampling interval is 0.002s and for analysis it is 0.004s, such that the mean of the particle in FOV to move at least one cell distance to avoid spurious velocities. MATPIV developed by Sveen (2003) has been used for the analysis. The comparison between the numerical (LS and CS) and the experimental measurement for velocity at the crest is shown in Fig.9. The CS velocity information is taken at the crest irrespective of the phase difference. The figure shows good comparison for velocity magnitudes using LS and EXP apart from H/d = 0.1, the reason stated above. The CS shows low velocity magnitude for H/d greater than 0.4. The spatial velocity information using PIV and numerical simulation (LS) for H/d = 0.5 is depicted in Fig.10.

5.0 Conclusion

In this study, the quantitative and qualitative analysis on phase difference between the numerical modeling based on Finite element method and experimental measurements are reported. The two approaches for estimating the horizontal velocities based on cubic spline and Least square method has been explored in detailed. The analysis has been carried out using the recent popular tool on time-frequency analysis based on Wavelets. The common high power has been shown using the Cross Wavelet transformation and phase lock behaviors are revealed using Wavelet Coherence. The analysis reveals that the cubic spline leads the experimental measurements for steep waves, showing the disadvantage when one applies to steep waves, where as, the Least square also leads the experimental measurements but the quantitative results are less when compared to the cubic spline. The Phase difference exists not at the primary period under investigation, but at the other modes. The phase difference is not constant at different locations of the tank; probable reason may be due to the uncertainty in the distance measurements of the wave gauges deployed in the laboratory. More precious measurement is mandatory. The solitary wave measurements and the comparison with the numerical modeling are reported along with the velocity information. Thus, Cubic spline and least square behavior are same for small steep waves, where as the least square approach shows promising for the medium to high steep waves. However, the errors are minimal, hence both these

methods are quite acceptable and the numerical modeling can be used as a replacement for physical modeling in certain circumstances.

6.0 References

Liu, P. C., 1994: Wavelet spectrum analysis and ocean wind waves. *Wavelets in Geophysics,* E. Foufoula-Georgiou and P. Kumar, Eds., Academic Press, 151–166.

Sriram V., Sannasiraj S.A., Sundar V., 2006, Numerical simulation of 2D nonlinear waves using finite element with cubic spline approximations, *Journal of Fluids and Structures*, 22(5), 663-681.

Torrence, C. and Compo, G. P., 1998, A practical guide to wavelet analysis, *Bulletin of American. Meteorological. Society*, 79, 61–78.

Meyers, S. D., B. G. Kelly, and J. J. O'Brien, 1993: An introduction to wavelet analysis in oceanography and meteorology: With application to the dispersion of Yanai waves. *Mon. Wea. Rev.,* **121,** 2858–2866.

Sveen J.K., http://www.math.uio.no/~jks/matpiv/ , 1998-2003.

Weng, H., and Lau, K.-M. 1994, Wavelets, period doubling, and time-frequency localization with application to organization of convection over the tropical western Pacific. *J. Atmos. Sci.,***51,** 2523–2541.

Daubechies, I., 1990, The wavelet transform time-frequency localization and signal analysis. *IEEE Trans. Inform. Theory,* **36,** 961–1004.

7.0 Publications during the period of study

Sriram, V., Sannasiraj S.A., Sundar V., Schlenkhoff A., Schlurmann T., (2008) "Experimental and Numerical Phase difference of a fully nonlinear free surface waves using Wavelet Approach", Proc. of Royal Society London Part A (Submitted).

Sriram,V., Sannasiraj,S.A., and Sundar,V., 2007," Wave-Structure interaction using unstructured FEM", *INCHOE 2007*.(In Press)

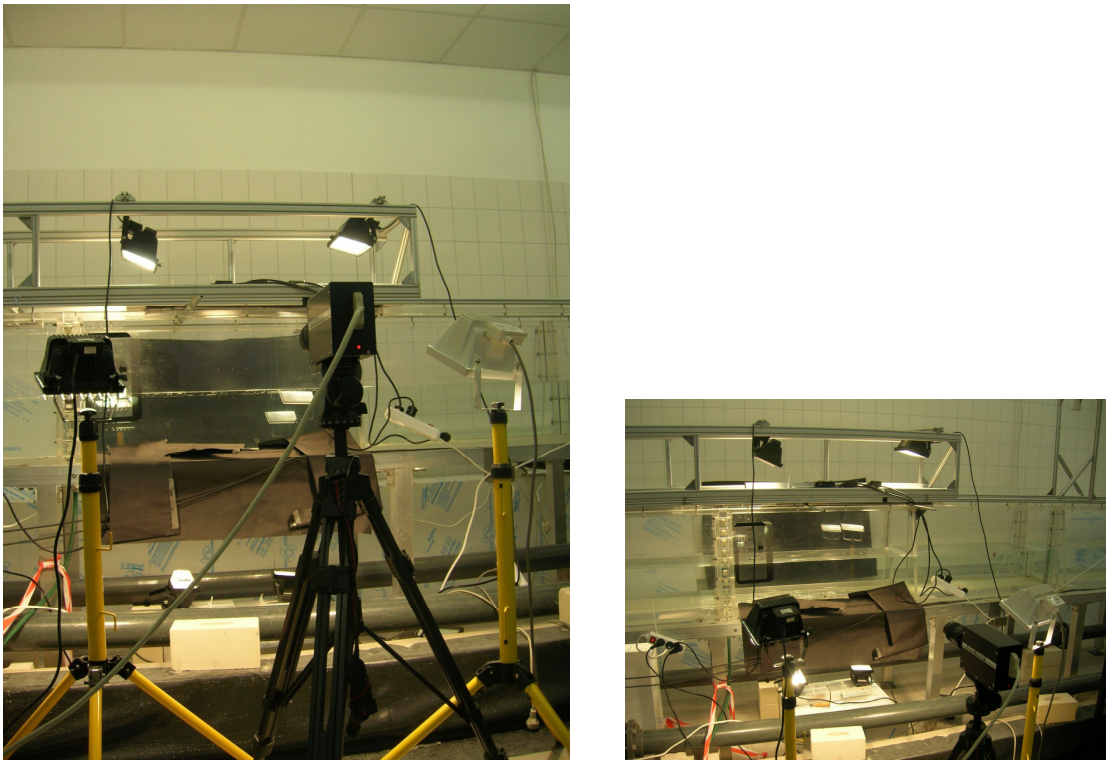

Fig.1. View of PIV setup.

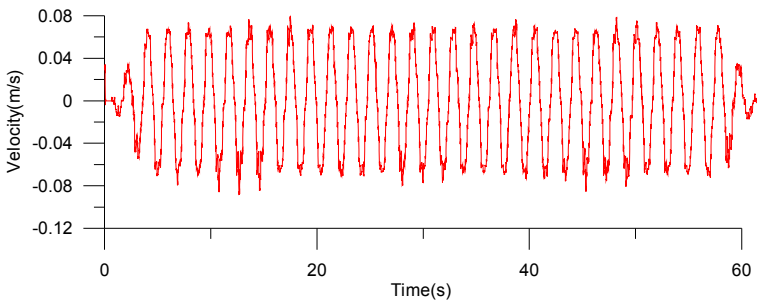

Fig.2a. Input velocity obtained from the paddle displacements.

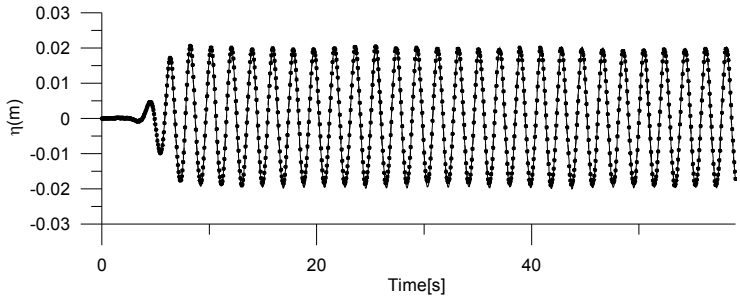

Fig.2b. Time history at 4.849m (dotted- EXP, Line- LS, dashed line-CS)

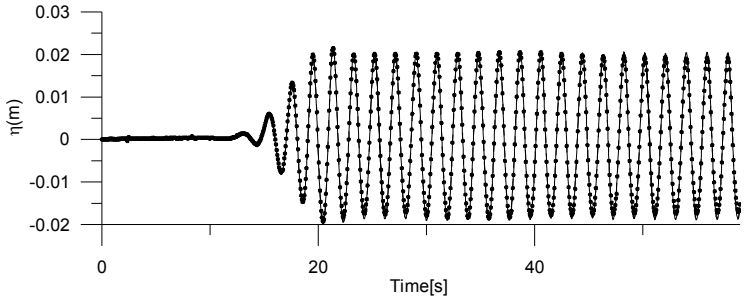

Fig.2c. Time history at 25.136m (dotted- EXP, Line- LS, dashed line-CS)

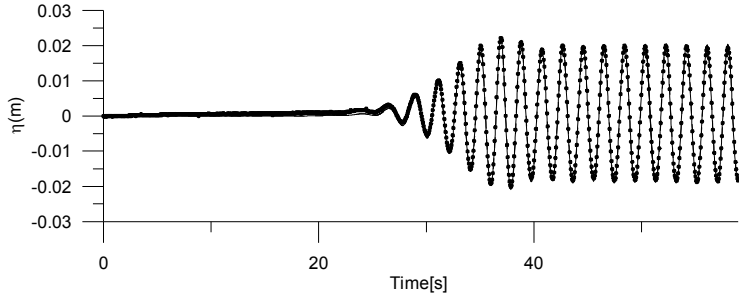

Fig.2d. Time history at 50.609m (dotted- EXP, Line- LS, dashed line-CS)

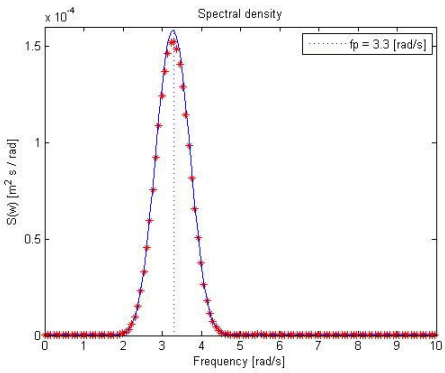

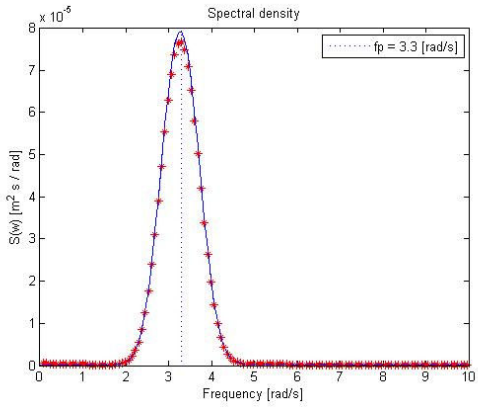

Fig.3a. Fourier spectrum for WP1.

Fig.3b. Fourier Spectrum for WP6 .

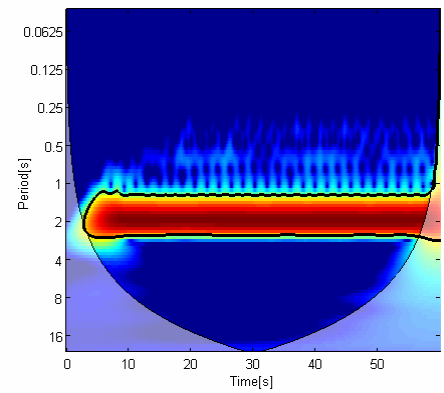

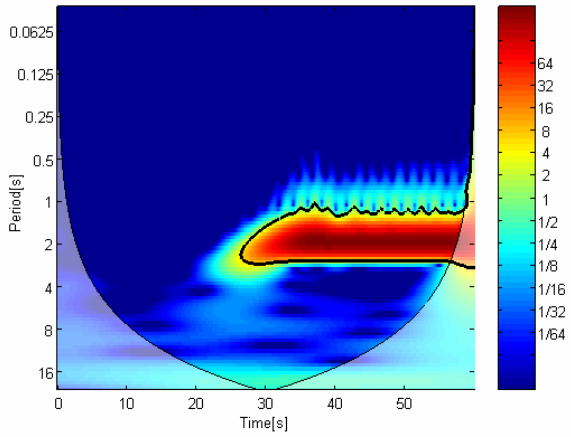

Fig.3c. Wavelet Power for EXP at WP1. Fig.3d. Wavelet Power for EXP at WP6.

Fig.3. Fourier and Wavelet Spectrum. WP1: 4.895m, WP6:50.609m. (dotted- EXP, Line- LS, dashed line-CS).

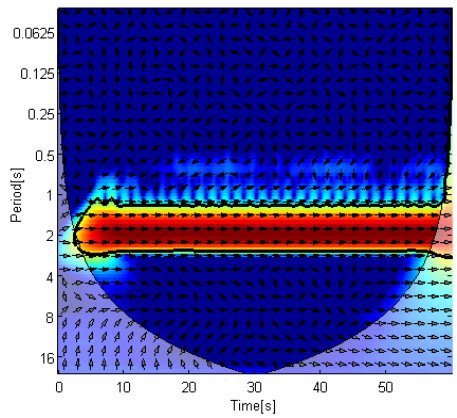

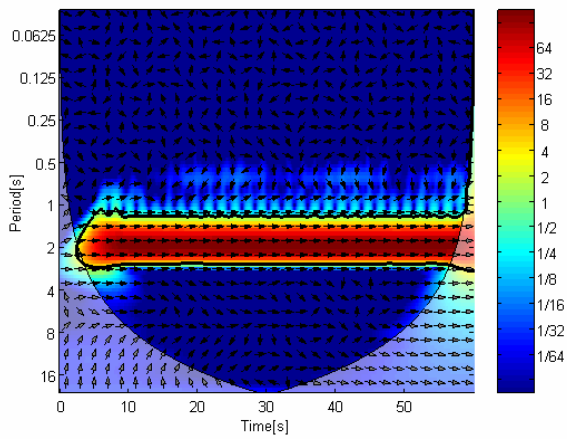

Fig.4a. Cross Wavelet between Exp-CS. Fig.4b. Cross Wavelet between Exp-LST.

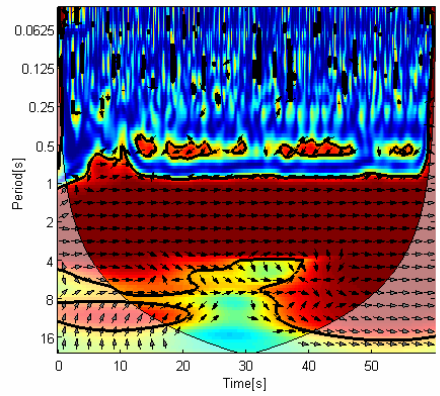

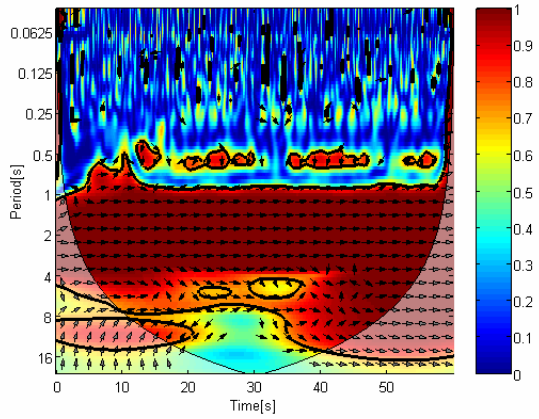

Fig.4c.Wavelet Coherence between Exp-CS. Fig.4d.Wavelet Coherence between Exp-LST.

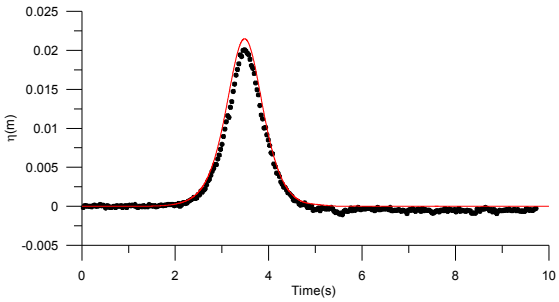

a) H/d = 0.1

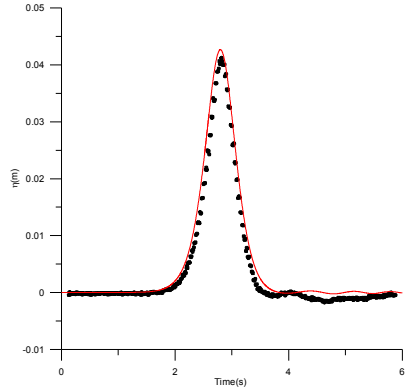

b) H/d = 0.2

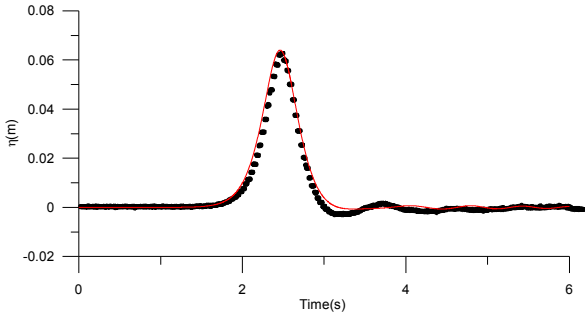

c) H/d = 0.3

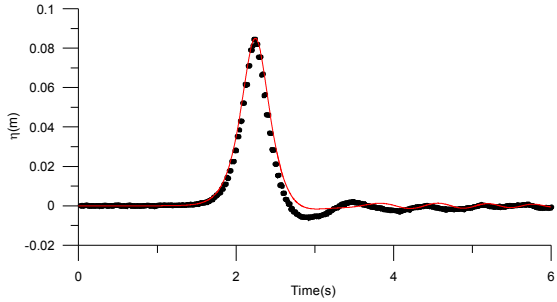

d) H/d = 0.4

Fig.5, Comparison between numerical (line) and experiments(dotted)

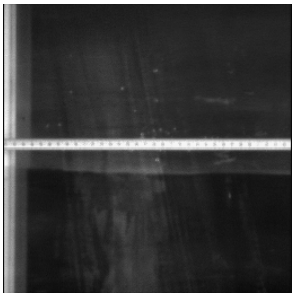

t = 0ms

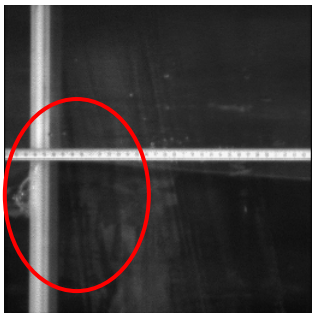

t = 248ms

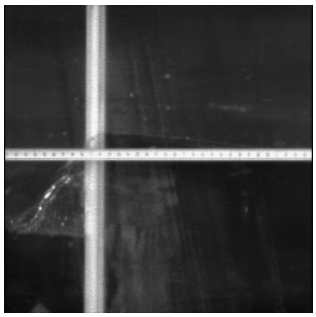

t = 344ms

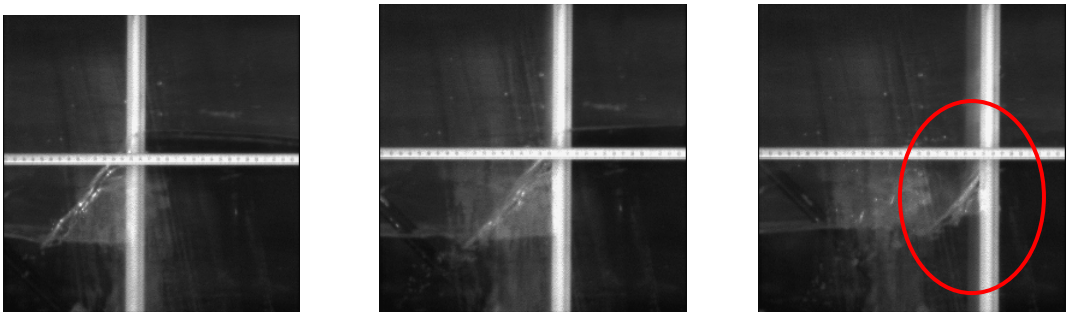

t = 498ms t = 684ms t = 897ms

Fig.6. Snap shots of the water flowing through the side walls.

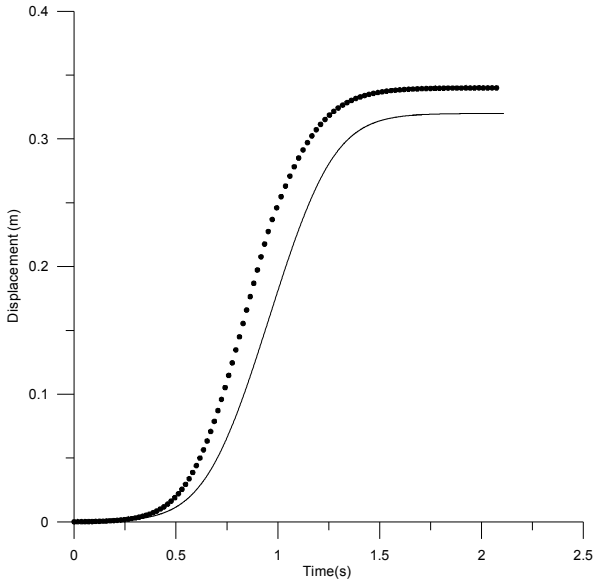

Fig.7. Showing the real signal (Line) and the input signal(dotted) to the paddle to generate same wave height(H/d = 0.1).

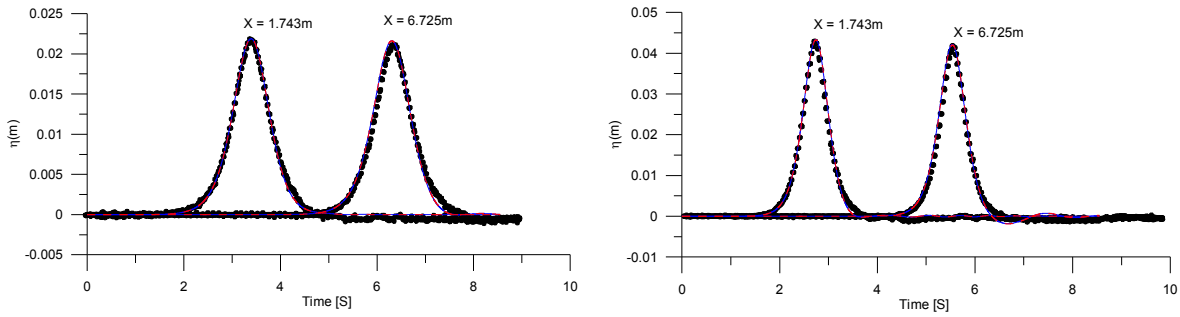

a) H/d = 0.1

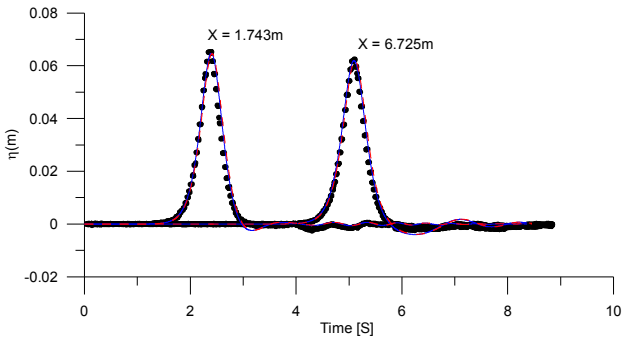

b) H/d = 0.2

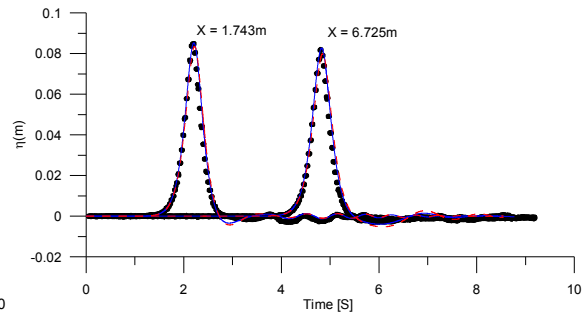

c) H/d = 0.3

d) H/d = 0.4

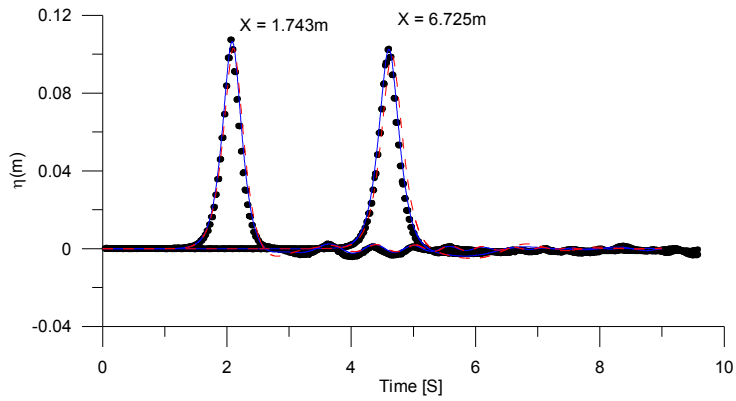

e) H/d = 0.5

Fig.8. Comparison of Time histories for Experiments (dotted), Least square (line), and Cubic spline (Dashed line)

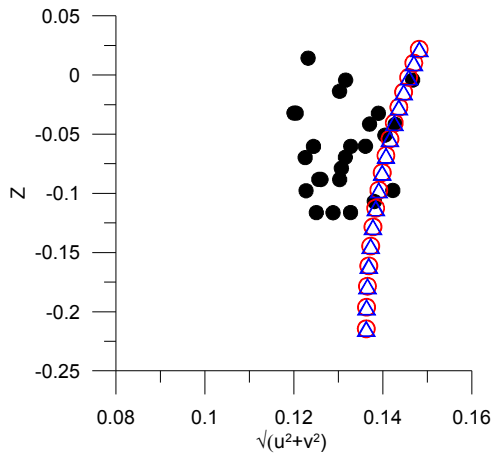

a) H/d =0.1

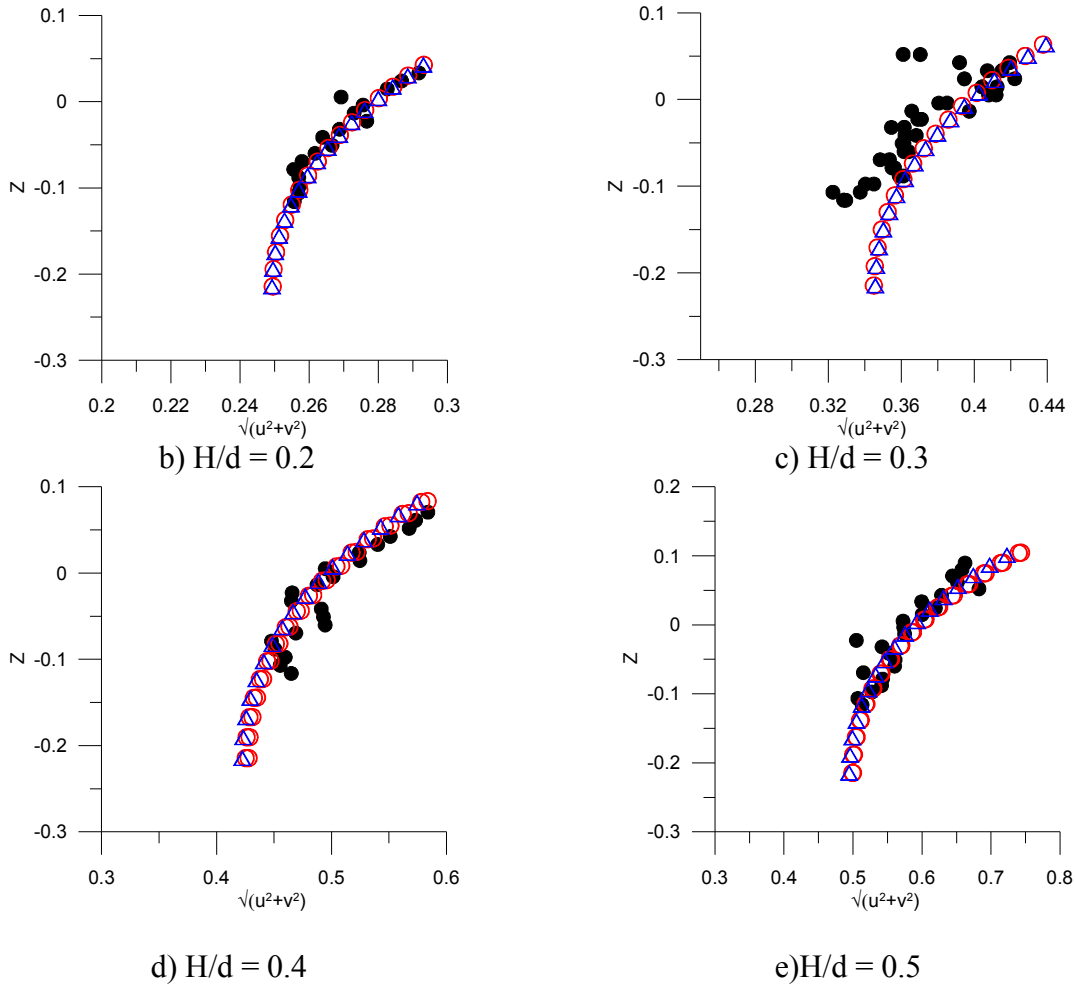

Fig.9. Velocity comparison between experiments(closed circle), least square (open circle) and Cubic spline(triangle)

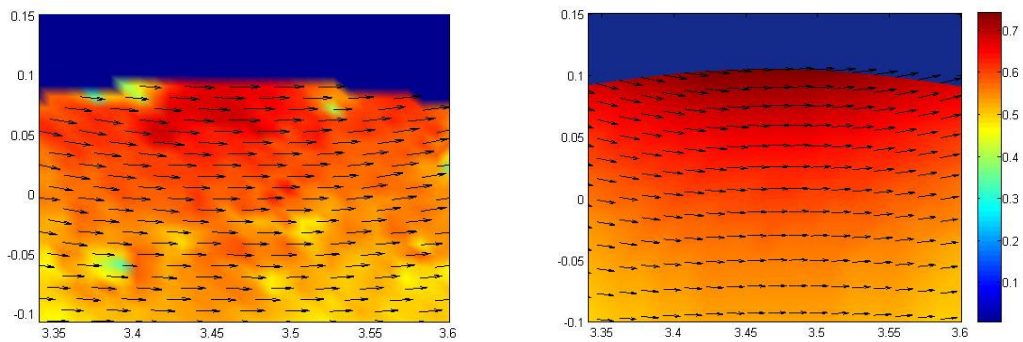

Fig.10. Spatial velocity information using experimental PIV measurement (left) and numerical simulation (right) for H/d = 0.5.

Table1. Quantitative Wavelet Phase difference between the numerical and experimental measurements at various locations along the length of the tank.

WP1 = 4.8495m, WP2 = 20.146m; WP3 = 25.136m; WP4 = 30.425m; WP5 = 40.406m; WP6 = 50.609m;

R- Regular Wave,CN- Cnoidal wave,CS- Cubic spline,LST-Least Square, XWT – Cross wavelet transform,WTC = Wavelet Coherence.

Type of wave	Numerical	Wavelet	WP 1 (in Deg)	WP2 (in Deg)	WP3 (in Deg)	WP4 (in Deg)	WP5 (in Deg)	WP6 (in Deg)
R1 T =1.92s, H = 0.04m D =0.613m	CS	XWT	-2.28±1.571	2.18±4.2173	1.71±6.057	3.59±1.8418	4.40±2.4762	1.05±2.1598
		WTC	-1.82±39.73	5.11±34.095	0.00±28.427	6.25±34.614	-2.68±39.10	3.01±36.582
	LST	XWT	-2.49±1.470	0.62±2.8111	0.28±4.9812	2.05±1.5636	2.44±1.8406	-1.40±1.9485
		WTC	-1.36±37.08	4.66±35.389	-1.06±29.002	5.36±32.115	-3.91±39.14	0.96±36.167
R2 T = 1.92s H = 0.2m D =0.621m	CS	XWT	-4.95±15.24	37.12±18.074	47.85±26.454	62.65±30.566	80.34±42.86	89.98±55.872
		WTC	1.38±26.517	14.81±35.984	30.20±42.565	30.09±51.889	29.96±72.41	37.1±77.24
	LST	XWT	-4.79±2.678	-3.76±8.108	-1.50±5.214	3.32±7.0019	8.91±4.7605	9.74±5.5117
		WTC	-2.11±24.05	-0.61±24.122	0.07±22.848	5.85±25.258	5.28±35.328	6.51±38.952
CN1 T = 6.4s H = 0.03m D =0.619m	CS	XWT	0.49±12.205	-2.24±14.22	-2.74±29.032	-1.42±23.446	-1.22±13.58	-4.38±6.3379
		WTC	-0.52±20.6	-2.62±22.42	-5.25±35.608	-1.56±22.039	-2.14±37.51	-0.96±23.05
	LST	XWT	0.51±12.26	-2.30±13.95	-2.74±28.99	-1.46±23.374	-1.28±13.52	-4.41±6.3277
		WTC	-0.51±19.19	-2.55±24.016	-5.68±37.036	-1.55±22.408	-1.85±38.45	-1.41±24.482
CN2 T = 6.4s H = 0.3m D =0.62m	CS	XWT	6.4±5.62	12.11 ±21.84	13.70 ±17.50	19.43±17.30	19.86±19.04	19.72 ±17.91
		WTC	8.04±25.61	8.88 ±26.83	10.91 ±30.77	13.30±32.74	14.44±33.44	12.87±33.19
	LST	XWT	1.59±3.3739	2.16±11.689	2.14±9.2675	3.59±7.5685	2.95±4.7214	0.57±4.0835
		WTC	4.29±21.473	2.07±22.606	3.36±26.222	3.59±27.065	2.60±25.94	1.06±25.951
CN3 T = 3.2s H = 0.2m D =0.621m	CS	XWT	3.19±4.4283	11.67±7.8744	12.00±6.5213	15.95±9.992	20.43±12.30	16.39±9.3233
		WTC	1.09±20.948	7.97±21.954	9.65±23.366	10.67±24.694	14.3±34.875	8.61±28.096
	LST	XWT	0.12±3.1459	1.49±2.8544	0.76±1.5744	5.71±4.6889	2.60±3.1248	-0.54±2.8526
		WTC	0.21±20.356	0.43±18.845	0.79±20.931	3.68±21.507	1.93±29.664	-1.00±26.033